Brillouin Lasing with a CaF_2 Whispering Gallery Mode Resonator

Ivan S. Grudinin,* Andrey B. Matsko,† and Lute Maleki†

Jet Propulsion Laboratory, California Institute of Technology, 4800 Oak Grove Drive, Pasadena, California 91109-8099, USA

(Received 25 February 2008; revised manuscript received 21 October 2008; published 28 January 2009)

Stimulated Brillouin scattering with both pump and Stokes beams in resonance with whispering gallery modes of an ultrahigh Q calcium fluoride resonator is demonstrated for the first time. The resonator is pumped with 1064 nm light and has 3 μW Brillouin lasing threshold. The scattering is observed due to the unique morphology of the resonator reducing the phase mismatch between the optical modes and the hypersound wave.

DOI: 10.1103/PhysRevLett.102.043902 PACS numbers: 42.60.Da, 42.65.Es, 42.70.Mp

Ultrahigh Q whispering gallery mode (WGM) microresonators [1,2] are commonly used to enhance the efficiency of the nonlinear optical processes such as three- [3,4] and four-wave mixing [5–7]. Strong spatial confinement of light as well as long interaction time of the light and the nonlinear medium provided by the resonators results in a significant decrease of the thresholds of both lasing [8,9] and stimulated Raman scattering [10–12].

Stimulated Brillouin scattering (SBS), one of the major nonlinear optical effects, is generally not observed in the ultrahigh-Q solid state microresonators even though the bulk Brillouin gain generally exceeds the Raman gain [13]. There are several reasons for this. There would be no WGM present at a Brillouin offset to support the Stokes beam. The SBS Stokes offset is generally around tens of GHz (20 GHz in silica [14], 18 GHz in fluorite [15]) and the gain bandwidth is only a few tens of MHz (100 MHz in silica [14] and 12 MHz in fluorite [15]), while the free spectral range (FSR) of WGM microresonators is hundreds of gigahertz and more. In addition, the acoustic frequency has to be resonant with one of the mechanical modes of the microresonator, otherwise the acoustic wave interferes destructively with itself. Finally, the pump mode, the Stokes mode, and the acoustic wave must have a nonvanishing overlap integral. Optical modes with close frequencies generally do not overlap in space. In crystals, speed of sound depends on direction and polarization of the wave, making it harder to fulfill the resonant conditions in the crystalline microresonators. This situation is alleviated in either fiber ring resonators, where FSR is small, or in low Q liquid microdroplets where optical resonance covers both pump and Stokes frequencies [13,16–21].

In this Letter we show that SBS takes place in the ultrahigh Q millimeter-scale WGM resonators which support two optical modes separated by the bulk SBS frequency shift. We predict that only the longitudinal sound wave is phase matched with the optical modes, present the first ever observation of an efficient SBS in a CaF_2 WGM resonator, and show that SBS can be either enhanced or suppressed by manipulating the modal structure of the optical resonator.

Let us first compute the expected Brillouin offset in a CaF_2 WGM resonator. We model the WGM as a toroid with axis along the (1,1,1) crystalline orientation (corresponding to the cut of the resonator we have fabricated). The phonon lifetime $\tau_{\rm ph} = \Gamma_B^{-1} \approx 0.08$ μs is inverse of the spectral width of the SBS gain, which is 12.2 MHz in fluorite [15]. The round-trip time of the sound wave in the resonator is $2\pi a/V_s = 2$ μs. Thus phonons do not form standing waves and SBS in millimeter-sized resonators is similar to scattering in bulk. To find the frequency offset of the SBS we need to know the direction of the light wave vector in the WGM with respect to the crystalline axes. The propagation direction of the electromagnetic wave is given by the following vector:

$$\mathbf{k} = \left(\frac{\cos\phi}{\sqrt{6}} - \frac{\sin\phi}{\sqrt{2}}, \frac{\cos\phi}{\sqrt{6}} + \frac{\sin\phi}{\sqrt{2}}, -\sqrt{\frac{2}{3}}\cos\phi\right), \quad (1)$$

where ϕ is the azimuth angle, representing different points along the resonator circumference. The geometry of our system allows backscattering only, so the Stokes beam has a wave vector $\mathbf{k}' \simeq -\mathbf{k}$. The wave vector for the phonons participating in the scattering is $\mathbf{q} = \mathbf{k}' - \mathbf{k}$, so the unit wave vector of the sound is $\vec{\kappa} = -\mathbf{k}$. CaF_2 is a cubic crystal described by three independent elastic constants. From the specifications of our fluorite sample we have: $C_{11} = 1.6420$, $C_{12} = 0.4398$, $C_{44} = 0.3370$ [$\times 10^{11}$ Pa]. Substituting these values into the set of equations presented in [22] we numerically find the frequency shifts of the Brillouin Stokes components as a function of angle ϕ for three different elastic waves (see Fig. 1). Computations were carried out in MATHEMATICA and MAPLE software packages. Only one solution has a frequency shift that depends weakly on the azimuth angle. The standard deviation is 40 MHz for this case, with 112 MHz peak-to-peak frequency change. The other two elastic waves have a standard deviation of frequency of about 400 MHz. Therefore, the 17.7 GHz branch has the maximum probability of exciting the stimulated process in the resonator. This prediction supports our experimental observations presented below. Further analysis shows that polarization

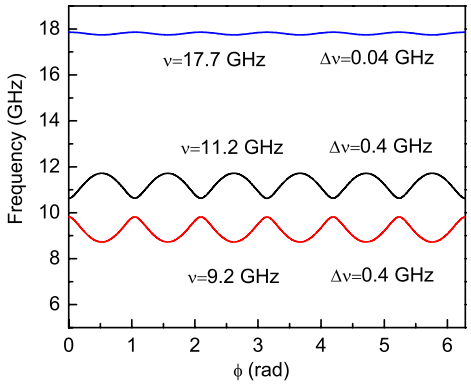

FIG. 1 (color online). Characteristic frequency of the Brillouin scattering as a function of the azimuth angle in a resonator. Frequencies of two tangential and one longitudinal (blue line on top) acoustic waves involved in Brillouin scattering are plotted for the fluorite resonator. Frequencies are changing for different points along the resonator's circumference (angle ϕ) due to varying orientation of the acoustic wave vector relative to the crystalline axes.

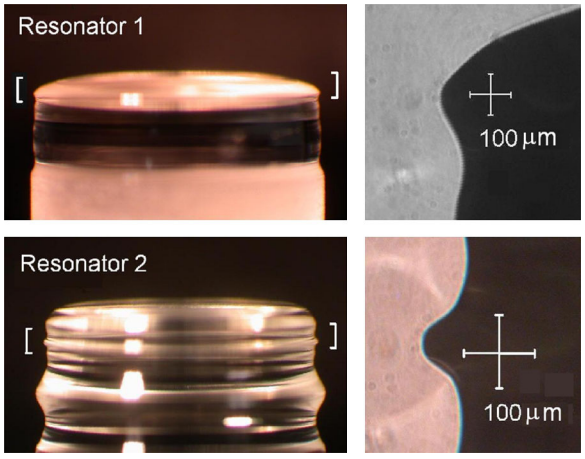

FIG. 2 (color online). Fluorite resonators. WGM localization areas are highlighted with the white brackets on the left. Shadow photographs of the highlighted regions are on the right. Diameters are 5.52 mm for resonator 1 and 5.21 mm for resonator 2.

of the phonons is nearly collinear with their wave vector in the case of the 17.7 GHz branch. Hence, the observed SBS process results from the interaction of light and longitudinal sound wave.

In the ideal case of spectrally singular pump and Stokes optical beams, the bulk Brillouin line-center gain g_b can be estimated as (see Eq. 8.3.24 of [23])

$$g_b = \frac{\gamma_e^2 \omega^2}{2\pi n V_s c^3 \rho \Gamma_B}, \tag{2}$$

where we assume that Stokes and pump wavelengths are equal: $\lambda_{Sj} = \lambda_p = 2\pi c/\omega$. The electrostrictive constant is $\gamma_e = [\rho(\partial\epsilon/\partial\rho)]_S \simeq 0.7$ [24], the fluorite refractive index at $\lambda = 1$ μm is $n = 1.429$, the density $\rho = 3.18$ g/cm^3, $\Gamma_B = 12.2$ MHz and the speed of sound is $V_s = [(C_{11} + C_{12} + 2C_{44})/(2\rho)]^{0.5} = 6.6 \times 10^5$ cm/s. Thus, the value of the bulk Brillouin gain for CaF_2 is equal to $g_B = 2.8 \times 10^{-9}$ cm/W and is 2 orders of magnitude larger than the bulk Raman gain $g_r = 2.4 \times 10^{-11}$ cm/W.

The SBS threshold power for the first Stokes line can be computed similarly to the Raman lasing case:

$$P_{\text{th}} = \frac{\pi^2 n^2}{g_b Q_p Q_{S1}} \frac{V}{\lambda_p \lambda_{S1}}. \tag{3}$$

Selecting realistic values for a 5 mm cavity, $V = 5 \times 10^{-6}$ cm^3, $Q_p = Q_{S1} = 10^9$, $\lambda_p = \lambda_{S1} = 1$ μm, we obtain $P_{\text{th}} \simeq 3.6$ μW.

To observe SBS we have fabricated two ultrahigh Q single-crystal CaF_2 WGM resonators, shown in Fig. 2. Resonator 1 was fabricated with a UV-grade fluorite from Edmund Optics and had a larger radius of curvature as compared to the resonator 2, which was made with an excimer-grade fluorite from Corning. A Nd:YAG laser with 5 kHz linewidth manufactured by Lightwave Electronics was used to excite WGMs at the wavelength of 1064 nm. The diameters of the resonators were determined from the FSR highlighted by multiple Raman Stokes lines observed at 1102 nm. The spectra of the resonators contain an abundance of WGMs with the average spacing of 25 MHz for both polarizations. We see such a dense WGM spectrum as well as a comparably large size of the resonators as the basic reason for the successful observation of the resonant SBS. The laser frequency was locked to a selected WGM using a simplified Pound-Drever-Hall technique. A signal generator was used to provide the excitation for the resonant phase modulator around 650 kHz. This signal was also used to synchronize the lock-in amplifier SR844 which operated as a frequency mixer and servo. This technique made it possible to maintain a fixed intracavity optical power.

Alignment of the angle-polished fiber couplers mounted onto the three-axis piezo positioning stages provided input and output coupling efficiencies of up to 80%. The light that was scattered backwards by the WGM was branched into the arm of a 90/10 fiber coupler. The setup schematically shown in Fig. 3 was used to measure the power and spectral properties of both forward and backward beams with a Yokogawa AQ6319 optical spectrum analyzer (OSA) and a Thorlabs detector DET10C. A WGM was excited with approximately 50 μW of optical power in a measurement conducted with the first resonator. The spectrum of light from coupler B [Fig. 4(a)] contains a Stokes line offset by 34.9 GHz and a weak Stokes line offset by 17.5 GHz. Neither stimulated Raman scattering (SRS) nor four-wave mixing oscillations were observed in this measurement. Two groups of Raman lines appeared around 1101.8–1102.3 nm and 1142.4–1142.9 nm as the pump power was further increased. A set of similar measure-

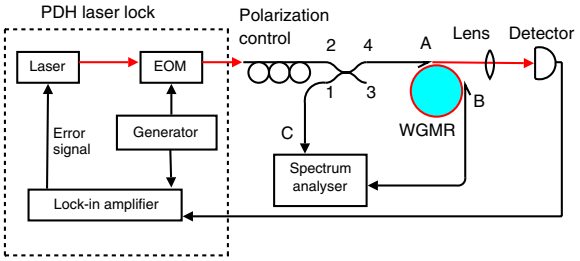

FIG. 3 (color online). Experimental setup diagram. Laser is locked to a WGM via simplified Pound-Drever-Hall technique. Optical power of clockwise and counterclockwise WG modes is monitored.

ments was performed with the second resonator. The excited WGM had a coupling efficiency of 70%, loaded Q factor of 4×10^9 and an intrinsic Q of around 1.4×10^{10}. The spectrum of the backscattered light is shown on Fig. 4(b). To determine threshold, pump power was reduced to 2.9 μW below which the first Stokes line was still present but weak. Above this power the intensity of the Stokes line jumps by around 10 dB and grows quickly with further pump increase. Hence, the threshold of the SBS is around 3 μW. At pump power well above 10 μW Raman lasing was observed in the second resonator as well. The Raman spectrum is shown on Fig. 5. For the second resonator we also carried out simultaneous measurements of the forward and backward optical spectrum using couplers B and C (Fig. 6). The asymmetry of the spectra may be explained by the residual power leakage between inputs 2 and 1 of the 90/10 coupler, increasing the backward signal at the pump wavelength. The spectra of our resonators had no observable resonance splitting, which means that only a minor amount of Rayleigh scattering is present for any given WGM. The excitation of a WGM at 1064 nm created a Stokes line offset by 17.5 GHz, which propagated in the direction opposite to the pump, as seen on the Fig. 4(b). This backscattered beam creates a cascaded Stokes component red-shifted by another 17.5 GHz propagating in the same direction as the pump beam [Fig. 4(a)]. A small feature at the double offset on Fig. 4(b) may be explained as Rayleigh scattering from the second Stokes line visible at Fig. 4(a). The weak feature at Fig. 4(a) may also be understood as Rayleigh scattering from the first Stokes line seen at Fig. 4(b). These two Stokes lines modify the Raman gain in the resonator, which leads to the SRS spectrum with modulated intensity as seen in the Fig. 5. Given the OSA resolution of 0.012 nm and the wavelength repeatability of 0.002 nm, or 1 GHz, we conclude that the two offsets of the observed Stokes lines are multiples of 17.7 GHz. This corresponds to Brillouin scattering by longitudinal phonon branch of fluorite, as shown above. The observation of the SBS in the WGM resonator is the main result of this Letter.

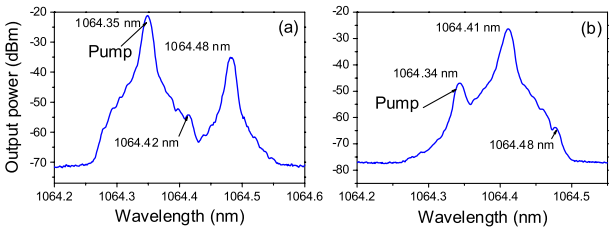

FIG. 4 (color online). (a) Output of the resonator 1, coupler B. Pump laser wavelength is 1064.35 nm. Low power at the spectrum analyzer is due to undercoupling. Frequency shift is 17.5 GHz for the weak Stokes and 35 GHz for the strong Stokes line. (b) Backward signal from output C for second resonator. Pump laser wavelength is 1064.34 nm. Stokes offset is 18 GHz for the first and 35.5 GHz for the second line. The width of each line is limited by the optical spectrum analyzer resolution of 0.012 nm.

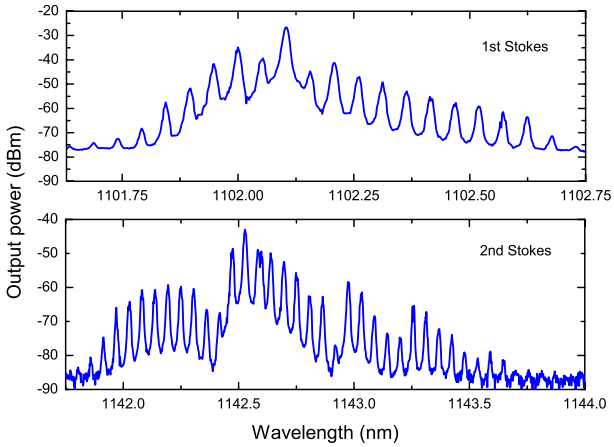

FIG. 5 (color online). Cascaded Raman lasing observed at pump power above 10 μW in the second cavity. Intensity modulation resembles Brillouin spectrum near the pump wavelength.

To show that the SBS was observed due to the specific shape of the WGM resonators, we have fabricated a single mode fluorite resonator [25] with Q factor approaching 10^9 and diameter of 5 mm. This resonator had an FSR of around 11 GHz, comparable with the FSR of the resonators we used to observe the Brillouin scattering. No modes were present at the Brillouin offset in the single mode resonator

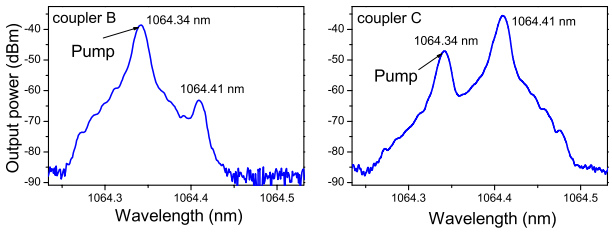

FIG. 6 (color online). Typical optical spectra from couplers B and C, representing forward and backward signals. Stokes offset is 17.7 GHz. Pump laser wavelength is 1064.34 nm. Spectrum analyzer resolution is 0.012 nm.

and no SBS was observed, as the result. Therefore, right selection of the resonator morphology allows us either to enhance or to suppress the scattering process.

We expect that the WGM Brillouin laser has an extremely narrow linewidth due to the high quality factor of the WGMs. Even though SBS is considered as lasing, it should be seen as a three-wave mixing process because of the long lifetime of the sound waves. In this mixing process the pump photon coherently decays into a phonon and the Stokes photon. Naturally, the phase diffusion of the Stokes wave depends on the phase diffusion of the optical pump. However, the narrow linewidth of the optical modes compared with the spectral width of the Brillouin gain allows suppressing this dependence significantly, so the linewidth of the Stokes beam becomes very narrow. The Stokes linewidth narrowing effect found in fiber-based Brillouin lasers [26] and the Schawlow-Townes limit may both be taken into account by introducing a Stokes beam phase diffusion coefficient D, defined as $\langle \phi^2 \rangle - \langle \phi \rangle^2 = Dt$. It can be shown, that D is given by

$$D = \frac{\Gamma_S^2}{(\Gamma_S + \Gamma_B)^2} D_P + \frac{\Gamma_S^2 \Gamma_B^2}{(\Gamma_S + \Gamma_B)^2} \frac{\hbar \omega_S}{4 P_S}, \qquad (4)$$

where Γ_S is the full widths at the half maximum of the Stokes WGM, D_P is the diffusion coefficient of the pump, P_S is the power of the Stokes beam leaving the resonator. We assume $D_P = 5$ kHz, $P_S = 1$ μW at the wavelength of 1 μm, and $\Gamma_S = 3$ kHz as recently demonstrated [27]. Under these conditions we expect the linewidth of the Stokes beam to be $D = 0.3 \times 10^{-3}$ Hz. At room temperature the linewidth will be limited by noises caused by temperature fluctuations in the resonator material.

It is worth noting that Brillouin scattering is different from the interaction of light and mechanical degrees of freedom of the optical cavity [28,29]. While mechanical modes of optical resonator are defined by its geometry, Brillouin frequency is defined by phase matching conditions, and depends on optical wavelength as well as on material elastic properties.

To the best of our knowledge, the first observation of an SBS in high-Q whispering gallery mode resonators was presented in this Letter. We have provided theoretical analysis verifying our experimental results. We argue that the observation of the doubly resonant SBS in miniature optical WGM resonators enables ultranarrow linewidth Brillouin lasers. The record high optical Q factor, mechanical stability and robustness of the crystalline WGM resonators make them naturally attractive elements for multiple applications.

The research described in this Letter was carried out at the Jet Propulsion Laboratory, California Institute of Technology, under a contract with the National Aeronautics and Space Administration, and support from DARPA MTO.

*Also at Applied Physics Department, California Institute of Technology, 1200 E. California Blvd., Pasadena, CA 91125, USA.
grudinin@caltech.edu

†Present address: Oewaves Inc., 1010 East Union Street, Pasadena, CA 91106, USA.

[1] K. J. Vahala, Nature (London) **424**, 839 (2003).
[2] A. B. Matsko and V. S. Ilchenko, IEEE J. Sel. Top. Quantum Electron. **12**, 3 (2006).
[3] V. S. Ilchenko *et al.*, Phys. Rev. Lett. **92**, 043903 (2004).
[4] M. Mohageg *et al.*, Opt. Express **13**, 3408 (2005).
[5] A. A. Savchenkov *et al.*, Phys. Rev. Lett. **93**, 243905 (2004).
[6] T. Carmon and K. J. Vahala, Nature Phys. **3**, 430 (2007).
[7] P. Del Haye *et al.*, Nature (London) **450**, 1214 (2007).
[8] H. B. Lin *et al.*, Opt. Lett. **11**, 614 (1986).
[9] V. Sandoghdar *et al.*, Phys. Rev. A **54**, R1777 (1996).
[10] H.-B. Lin and A. J. Campillo, Phys. Rev. Lett. **73**, 2440 (1994).
[11] S. M. Spillane, T. J. Kippenberg, and K. J. Vahala, Nature (London) **415**, 621 (2002).
[12] I. S. Grudinin and L. Maleki, Opt. Lett. **32**, 166 (2007).
[13] P. T. Leung and K. Young, Phys. Rev. A **44**, 593 (1991).
[14] A. Debut, S. Randoux, and J. Zemmouri, J. Opt. Soc. Am. B **18**, 556 (2001).
[15] T. Sonehara *et al.*, J. Opt. Soc. Am. B **24**, 1193 (2007).
[16] J.-Z. Zhang and R. K. Chang, J. Opt. Soc. Am. B **6**, 151 (1989).
[17] S. M. Chitanvis and C. D. Cantrell, J. Opt. Soc. Am. B **6**, 1326 (1989).
[18] A. L. Huston, H.-B. Lin, J. D. Eversole, and A. J. Campillo, Opt. Lett. **15**, 1176 (1990).
[19] J.-Z. Zhang, G. Chen, and R. K. Chang, J. Opt. Soc. Am. B **7**, 108 (1990).
[20] S. C. Ching, P. T. Leung, and K. Young, Phys. Rev. A **41**, 5026 (1990).
[21] C. D. Cantrell, J. Opt. Soc. Am. B **8**, 2158 (1991); **8**, 2181 (1991).
[22] I. Fabelinskii, *Molecular Scattering of Light* (Plenum Press, New York, 1968).
[23] *Nonlinear Optics*, edited by R. Boyd (Academic Press, New York, 1992).
[24] H. Mueller, Phys. Rev. **47**, 947 (1935).
[25] A. A. Savchenkov *et al.*, Opt. Lett. **31**, 1313 (2006).
[26] J. Geng *et al.*, IEEE Photonics Technol. Lett. **18**, 1813 (2006).
[27] A. A. Savchenkov *et al.*, Opt. Express **15**, 6768 (2007).
[28] T. J. Kippenberg and K. J. Vahala, Opt. Express **15**, 17172 (2007).
[29] T. J. Kippenberg and K. J. Vahala, Science **321**, 1172 (2008).